International Journal of Thermodynamics (IJoT)
ISSN 1301-9724 / e-ISSN 2146-1511
https://dergipark.org.tr/en/pub/ijot

Vol. xx (No. x), pp. xxx-xxx, 2024
doi: 10.5541/ijot.1458027
Published online: Month dd, 2024

Research Article

Thermodynamic Optimization and Energy-Exergy Analyses of the Turboshaft Helicopter Engine

[1]M. Siyahi, [2]*H. Siyahi, [3]M. Fallah, [4]Z. Mohammadi

[1,2] Department of Aeronautical Engineering, Istanbul Technical University -Turkey
[3,4] Mechanical Engineering Department, Azarbaijan Shahid Madani University -Iran
E-mails: [1]siyahi20@itu.edu.tr, [2]*siyahi16@itu.edu.tr, [3]mfallah@azaruniv.ac.ir, [4]zahra_mohammadij@yahoo.com

Received 30 March 2024, Revised 11 May 2024, Accepted 7 July 2024

Abstract

Energy demand is a critical contemporary concern, with significant implications for the future. While exploring renewable or sustainable energy sources offers potential solutions, optimizing energy consumption in existing power generation systems is also key. Aviation accounts for a substantial portion of energy demand, underscoring the importance of energy efficiency in this sector. Conventional energy analyses may be misleading; hence, employing exergy-based analyses provides a clearer understanding of energy consumption. Also, most of these analyses do not include the effect of the turbine blade's cooling in calculations. In the present study, exergy analyses have been conducted on a helicopter turboshaft engine with turbine-blades cooling, focusing on design parameters such as ambient temperature, compressor pressure ratio, and turbine inlet temperature. Thermodynamic optimizations are conducted using a genetic algorithm. Results show that increasing pressure ratio and turbine inlet temperature boost performance, yet technical restrictions on compressor and turbine size, and metallurgical constraints on turbine blades' material limit these gains. Sea level scenario prioritizes ambient temperature-drop for enhancing net-work and efficiency, while altitude-gain boosts turboshaft performance. Combustion chambers incur the highest exergy destruction of 74-80%, followed by 16-20% and 4-6% exergy destructions in the turbine and compressor, respectively. Lower air temperatures and higher flight altitudes demand larger fuel consumption for equivalent turbine inlet temperature, albeit enhancing cooling capacity and reducing required cooling air fraction for turbine blades.

Keywords: *Turboshaft engine; energy-exergy analyses; thermodynamic optimization; energy efficiency; exergy efficiency; exergy destruction.*

1. Introduction

A turboshaft engine is an engine type that is designed to generate shaft power rather than jet thrust. This type of engine is widely used for applications that require large power with a lightweight and small size. Turboshaft engines are widely used in helicopters, hovercrafts, tanks, boats, and ships [1, 2]. Because of the huge usage of turboshaft engines in helicopters, it worth paying special attention to the performance analysis of this engine type via energy efficiency and optimization [3-5]. Energy can be explained in two parts, exergy is the maximum accessible work or potential work and anergy is a part that cannot be benefited from. In other words, exergy is the quality of energy and can be expressed as how good we are or can be using an energy source. Exergy analysis is a practical and powerful tool for performance analysis [6]. Many engineers and scientists suggest that exergy analysis is a highly effective method for evaluating and enhancing thermodynamic performance, and is superior to energy analysis [7]. Many researchers have investigated aircraft engines and propulsion systems using exergy analysis [8-17]. Others examine the importance of defining a reference environment that varies with altitude and applying that work to a turbojet engine [18, 19]. Many have applied parametric studies based on different ambient and operating parameters along with exergy methods to analyze the performance of an aircraft engine [20-22]. Besides, the parametric studies can give a good understanding of the performance change of aircraft engines in different ambient and design situations. The other research explains that the ambient air pressure and temperature, compressor pressure ratio, turbine inlet temperature, and the efficiency of components are the most important parameters that influence the performance of the gas turbine cycle [23]. Recent studies have applied the exergy analysis to optimize the performance of aircraft propulsion systems [24]. While some studies address the optimization of the cruise velocity of an aircraft [3], others investigate the engine configuration optimization methods [25]. One of the most beneficial impacts of exergy analysis is that it can be utilized for economic assessments [26]. They develop several parameters such as thrust cost rate, cost of exergy destruction, relative cost difference, and exergoeconomic cost to calculate the thrust cost rate. Moreover, exergy analyses can be a useful tool for studying environmental effects [27]. The authors of the present study have noticed that there is a gap in the literature studying turboshaft engines from the 2nd law of thermodynamics point of view which includes turbine cooling. The main focus of the present research work is on the parametric study, exergy analysis, and thermodynamic optimization of a turboshaft helicopter

*Corresponding Author

engine equipped with a practical model for turbine blades' cooling.

2. Governing Equations

All explanations for energy and exergy analyses are explained in detail in Appendix A and Appendix B. Noticing that 1, 2, 3, and 4 states respectively introduce the compressor inlet, combustion chamber inlet (compressor outlet), turbine inlet (combustion chamber outlet), and exhaust (turbine outlet) in Figure 1, the simplified equations for thermodynamic analyses of different components of the turboshaft engine are revealed in the following sections.

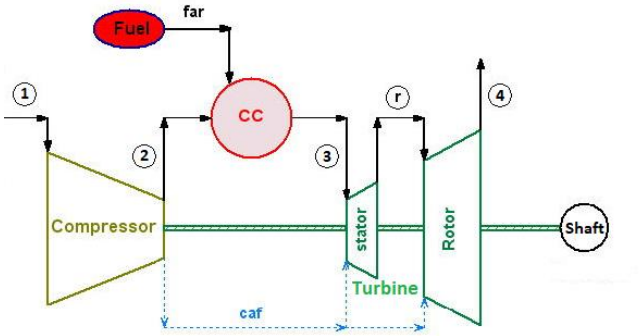

Figure 1. Schematic of turboshaft-engine configuration.

2.1 Polytropic Compressor

Considering the definition of the compressor's polytropic efficiency, it can be written as [28-32]:

$$\eta_{poly,comp}=\frac{\bar{R}T\frac{dP}{P}}{\bar{C}_{p,air}dT} \tag{1}$$

which the molar specific heat coefficient of air at constant pressure based on its elements is [33-38]:

$$\bar{C}_{p,air}=\frac{\Sigma(n_i\bar{C}_{p,i})_{air}}{\Sigma(n_i)_{air}} \tag{2}$$

By integrating equation (1) the compressor outlet temperature (COT=T2) can be calculated as:

$$\int_{T_1}^{T_2}\bar{C}_{p,air}\frac{dT}{T}=\int_{P_1}^{P_2}\frac{\bar{R}}{\eta_{poly,comp}}\frac{dP}{P} \tag{3}$$

Mass conservation for compressor, [33-38] is:

$$\dot{m}_1=\dot{m}_2+(caf)\dot{m}_1 \tag{4}$$

Energy conservation for compressor, [33-38] is:

$$\dot{W}_{comp}+\dot{m}_1 e_1=\dot{m}_1 e_2 \tag{5}$$

The exergy balance for the compressor can be written as, [33-38]:

$$\dot{W}_{comp}+\dot{m}_1 ex_1=\dot{m}_1 ex_2+\dot{E}x_{D,comp} \tag{6}$$

The exergy efficiency of the compressor is [33-38]:

$$\eta_{II,comp}=\frac{(\dot{W}_{comp}-\dot{E}x_{D,comp})}{\dot{W}_{comp}}100 \tag{7}$$

2.2 Combustion Chamber

After the compressor, air enters the combustion chamber as an oxidizer with a molar ratio of 21% oxygen and 79% nitrogen. The combustion process is carried out assuming that nitrogen does not participate in the reaction. The reaction equation considering the factor of excess air (λ) can be calculated as, [28-32]:

$$\begin{aligned}&C_nH_m+\lambda\left(n+\tfrac{m}{4}\right)[O_2+3.76N_2+(4.76\bar{\omega}_1)H_2O]\Rightarrow\\&(n)CO_2+(\lambda\text{-}1)\left(n+\tfrac{m}{4}\right)O_2+\\&3.76\lambda\left(n+\tfrac{m}{4}\right)N_2+\left[\lambda\left(n+\tfrac{m}{4}\right)(4.76\bar{\omega}_1)+\tfrac{m}{2}\right]H_2O\end{aligned} \tag{8}$$

with the assumption of an adiabatic combustion process, the energy conservation for the combustion process is as follows [28-32]:

$$\sum(n_i\bar{h}_i)_{Reactants}=\sum(n_i\bar{h}_i)_{Products} \tag{9}$$

which the enthalpy of ith element ($\bar{h}_i$) is:

$$\bar{h}_i=\bar{h}_f^0+\int_{298.15}^{T}\bar{C}_p dT \tag{10}$$

The energy equation of combustion can be rewritten as:

$$\begin{aligned}&\int_{298.15}^{T_f}\bar{C}_{p,C_nH_m}dT+\lambda\left(n+\tfrac{m}{4}\right)\int_{298.15}^{T_2}\bar{C}_{p,O_2}dT+\\&\lambda\left(n+\tfrac{m}{4}\right)3.76\int_{298.15}^{T_2}\bar{C}_{p,N_2}dT+\\&\lambda\left(n+\tfrac{m}{4}\right)4.76\bar{\omega}_1\int_{298.15}^{T_2}\bar{C}_{p,H_2O}dT=\\&n\int_{298.15}^{TIT}\bar{C}_{p,CO_2}dT+(\lambda\text{-}1)\left(n+\tfrac{m}{4}\right)\int_{298.15}^{TIT}\bar{C}_{p,O_2}dT+\\&3.76\lambda\left(n+\tfrac{m}{4}\right)\int_{298.15}^{TIT}\bar{C}_{p,N_2}dT+\\&\left[\lambda\left(n+\tfrac{m}{4}\right)(4.76\bar{\omega}_1)+\tfrac{m}{2}\right]\int_{298.15}^{TIT}\bar{C}_{p,H_2O}dT\end{aligned} \tag{11}$$

alternatively, by knowing the turbine inlet temperature (TIT) and solving energy conservation for combustion chamber the excess air (λ) is calculated. Consequently, by knowing the λ and the efficiency of the combustion chamber ($\eta_{I,cc}$), the fuel-air ratio (far) is calculated as:

$$far=\frac{M_{C_nH_m}}{\lambda\left(n+\frac{m}{4}\right)4.76(1+\bar{\omega}_1)M_{air}\eta_{I,cc}}(1\text{-}caf) \tag{12}$$

Mass conservation for combustion chamber [33-38]:

$$\dot{m}_2+\dot{m}_f=\dot{m}_3 \tag{13}$$

which fuel mass ($\dot{m}_f$) equals:

$$\dot{m}_f=(far)\dot{m}_1 \tag{14}$$

The exergy balance for the combustion chamber is given as [33-38]:

$$\dot{m}_2 ex_2+\dot{m}_f ex_f=\dot{m}_3 ex_3+\dot{E}x_{D,cc} \tag{15}$$

and the exergy efficiency for combustion can be written as [33-38]:

$$\eta_{II,cc}=\left[1-\frac{\dot{E}x_{D,cc}}{(far)\dot{m}_1 ex_f}\right]100 \tag{16}$$

2.3 Cooling Air Fraction (caf) of Turbine Blades

To simulate the turboshaft engine more realistically, it is assumed that turbine has one stationary and one rotary stage and a cooling method that gives a simple relationship between turbine inlet temperature (TIT) and the rotor inlet temperature (T_r) is applied for turbine blades as [39-41]:

$$T_r=0.8451(TIT)+136.2 \tag{17}$$

which the temperatures are in degrees Celsius.

Mass conservation for stationery blades stage is as:

$$\dot{m}_3+\left(\frac{caf}{2}\right)\dot{m}_1=\dot{m}_r \tag{18}$$

replacing equation 13 in equation 18, $\dot{m}_r$ can be rewritten as:

$$\dot{m}_r=\left(1-\frac{caf}{2}+far\right)\dot{m}_1 \tag{19}$$

Energy conservation for stationary blades is:

$$\dot{m}_3 e_3+\left(\frac{caf}{2}\right)\dot{m}_1 e_2=\dot{m}_r e_r \tag{20}$$

by replacing equations 13 and 19 in equation 20 the energy equation will be as:

$$(1-caf+far)\dot{m}_1 e_3+\left(\frac{caf}{2}\right)\dot{m}_1 e_2=\left(1-\frac{caf}{2}+far\right)\dot{m}_1 e_r \tag{21}$$

after simplification, the cooling air fraction (caf) can be calculated as:

$$caf=\frac{2(1+far)(e_3-e_r)}{(2e_3-e_2-e_r)} \tag{22}$$

2.4 Polytropic Turbine

Considering the definition of the turbine's polytropic efficiency, it can be written as [28-32]:

$$\eta_{poly,turb}=\frac{\bar{C}_{p,g}dT}{\bar{R}T\frac{dP}{P}} \tag{23}$$

which the molar specific heat coefficient of products at constant pressure based on its elements is [33-38]:

$$\bar{C}_{p,g}=\frac{\Sigma(n_i\bar{C}_{p,i})_{product}}{\Sigma(n_i)_{product}} \tag{24}$$

By integrating equation (23) the turbine outlet temperature (TOT = T_4) can be calculated as:

$$\int_{T_r}^{TOT}\bar{C}_{p,g}\frac{dT}{T}=\int_{P_3}^{P_4}\eta_{poly,turb}\bar{R}\frac{dP}{P} \tag{25}$$

Mass conservation for turbine is [33-38]:

$$\dot{m}_3+(caf)\dot{m}_1=\dot{m}_4 \tag{26}$$

The Energy conservation for turbine is [33-38]:

$$\dot{m}_3 e_3+(caf)\dot{m}_1 e_2=\dot{m}_4 e_4+\dot{W}_{turb} \tag{27}$$

The exergy balance equation for the turbine can be written as [33-38]:

$$\dot{m}_3 ex_3+(caf)\dot{m}_1 ex_2=\dot{m}_4 ex_4+\dot{W}_{turb}+\dot{E}x_{D,turb} \tag{28}$$

The exergy efficiency of the turbine is as [33-38]:

$$\eta_{II,turb}=\frac{\dot{W}_{turb}}{(\dot{W}_{turb}+\dot{E}x_{D,turb})}100 \tag{29}$$

2.5 Energy-Exergy Analysis of the Entire Cycle

Considering the special mechanical efficiency (η_{mech}), the cycle net work is [33-38]:

$$\dot{W}_{net}=(\dot{W}_{turb}-\dot{W}_{comp})\eta_{mech} \tag{30}$$

By using the low heat value (LHV) of the fuel, the thermal efficiency of the cycle (energy efficiency) can be expressed as follows [33-38]:

$$\eta_{I,cycle}=\frac{\dot{W}_{net}}{(far)\dot{m}_1\ LHV}100 \tag{31}$$

According to the equations mentioned in the previous sections and chapter, the exergy balance for the entire gas turbine cycle can be written as follows, [33-38]:

$$\dot{m}_1 ex_1+\dot{m}_f ex_f=\dot{m}_4 ex_4+\dot{W}_{net}+\dot{E}x_{D,cycle} \tag{32}$$

The irreversibility of the entire system can be considered as the summation of the exergy destructions of individual components of the cycle [33-38]:

$$\dot{I}_{D,cycle}=\dot{E}x_{D,cycle}=\dot{E}x_{D,comp}+\dot{E}x_{D,cc}+\dot{E}x_{D,turb} \tag{33}$$

Finally, the exergy efficiency of entire cycle can be obtained as [33-38]:

$$\eta_{II,cycle}=\frac{\dot{W}_{net}}{(far)\dot{m}_1\ ex_f}100 \tag{34}$$

All required equations for the energy-exergy analyses and thermodynamic optimization of the turboshaft engine have been summarized in Appendix C.

3. Mathematical Method

The genetic method is a robust optimization algorithm that is designed to reliably locate a global optimum even in the presence of local optima. The genetic method implemented in the engineering equation solver (EES) program is derived from the public domain Pikaia optimization program (version 1.2) written by Paul Charbonneau and Barry Knapp at the National Center for Atmospheric Research (NCAR). A detailed explanation of genetic optimization algorithms in general and specific details of the Pikaia program are provided in [42].

The genetic method intends to mimic the processes occurring in biological evolution. A population of individuals (sample points) is initially chosen at random from the range specified by the bounds of the independent variables. The individuals in this population are surveyed to determine their fitness (the values of the objective function as quantified by the value of the variable that is to be minimized or maximized). Then a new generation of individuals is generated in a stochastic manner by 'breeding' selected members of the current population. The characteristics of an individual that are passed on to the next generation are represented by encoded values of its independent variables. The probability that an individual in the current population will be selected for breeding the next generation is an increasing function of its fitness. The

'breeding' combines the characteristics of two parents in a stochastic manner. Additional random variations are introduced by the possibility of 'mutations' for which the offspring may have characteristics that differ markedly from those of the parents. In the current implementation, the number of individuals in the population remains constant for each generation.

The three parameters in the genetic method that are most responsible for identifying an optimum and for the associated computing effort are the number of individuals in a population, the number of generations to explore, and the maximum mutation rate.

Unlike the Conjugate Directions and Variable Metric methods, the genetic method is not affected by the guess values of the independent parameters. However, the lower and upper bounds on the independent parameters are extremely important since the initial population and subsequent stochastic selections are chosen from within these bounds.

4. Results

In the present study, the performance analyses of a turboshaft engine cycle equipped with turbine blades' cooling are carried out via the engineering equation solver (EES) program.

The energy-exergy analyses have been done with the parametric studies of turboshaft engine's specific net-work (w_{net}), energy efficiency (η_I), and exergy efficiency (η_{II}) with respect to different ambient conditions and different operating conditions. The metallurgical and technological considerations limit the maximum turbine inlet temperature and pressure ratio of the TIT=1200℃ and r_p=35 for the turboshaft engines.

A typical maximum flight altitude of 9 km has been specified for the helicopter engine.

The thermodynamic optimizations have been performed through maximization of w_{net}, η_I and η_{II} by using the genetic algorithm technique.

The fuel used in turboshaft engine is "Kerosene or Dodecane" with the chemical formula of $C_{12}H_{26}$ which is considered to be the most common fuel used in today's jet engines.

It is assumed that turboshaft engine works at steady state steady flow (SSSF) condition.

4. 1 Validation

A program has been written for an open simple gas turbine cycle and results have been compared with reference data [23] in Table 1.

Table 1. The Validation Table of EES Program Results vs. Results of Reference, [23].

Variables	Reference	Present Study	Deviation
T_{amb}	15 ℃	15 ℃	**0.0 %**
P_{amb}	101 kPa	100 kPa	**0.1 %**
RH_{amb}	60 %	60 %	**0.0 %**
$\eta_{poly,comp}$	92 %	92 %	**0.0 %**
$\eta_{poly,turb}$	86 %	89 %	**3.5 %**
η_{mech}	99.5 %	100 %	**0.5 %**
$r_{p,comp}$	20	20	**0.0 %**
COT	449.6 ℃	438.6 ℃	**2.4 %**
TIT	1331.3 ℃	1330 ℃	**0.1 %**
TOT	620 ℃	617.1 ℃	**0.5 %**
$\eta_{I,cycle}=\eta_{thermal,cycle}$	40.16 %	40.08 %	**0.2 %**

It could be clearly figured out that the maximum deviation of the calculated results is 3.5%, which is reasonable for a parametric study.

4. 2 Turboshaft Engine

It is assumed that ambient relative humidity (RH_{amb}=15%) and operating turbine inlet temperature (TIT=1200 ℃) are constant for all cycles. The thermodynamics optimization and energy-exergy analyses have been done for a turboshaft engine in different air temperatures and altitudes.

At sea level, results show that decreasing the temperature of air leads to an increase in the density. Since a compressor works with the same volumetric flow rate, by increasing the air density, the inlet air mass flow rate increases. Moreover, the fuel-air ratio increases to reach the same turbine inlet temperature, consequently, the entire cycle mass flow rate increases. Therefore, for the same turbine inlet temperature decrease at the compressor inlet temperature will increase the specific net-work of the turboshaft engine (Table 2).

Table 2. Optimization of the Performance of the Turboshaft Engine Cycle for the Maximum Specific Work (w_{net}) at Sea Level, RH_{amb}=15%, TIT=1200 ℃ and Different Ambient Temperatures.

T_{amb} [℃]	TIT [℃]	Design Parameters	Values
10	1200	$r_{p.comp}$	18.13
		far [kg/kg]	0.01936
		caf [kg/kg]	0.1285
		λ (excess air fraction)	3.052
		$w_{net,max}$ [kJ/kg]	**341.8**
25	1200	$r_{p.comp}$	16.46
		far [kg/kg]	0.01903
		caf [kg/kg]	0.1303
		λ (excess air fraction)	3.093
		$w_{net,max}$ [kJ/kg]	**321.6**
40	1200	$r_{p.comp}$	16.46
		far [kg/kg]	0.01829
		caf [kg/kg]	0.1347
		λ (excess air fraction)	3.187
		$w_{net,max}$ [kJ/kg]	**303**

Table 3. Optimization of the Performance of the Turboshaft Engine Cycle for the Maximum Thermal Efficiency ($\eta_{I,cycle,max}$) at Sea Level, RH_{amb}=15%, TIT=1200 ℃ and Different Ambient Temperatures.

T_{amb} [℃]	TIT [℃]	Design Parameters	Values
10	1200	$r_{p.comp}$	34.99
		far [kg/kg]	0.01596
		caf [kg/kg]	0.149
		λ (excess air fraction)	3.614
		$\eta_{I,cycle,max}$	**46.68**
25	1200	$r_{p.comp}$	34.99
		far [kg/kg]	0.01499
		caf [kg/kg]	0.1563
		λ (excess air fraction)	3.806
		$\eta_{I,cycle,max}$	**45.42**
40	1200	$r_{p.comp}$	34.99
		far [kg/kg]	0.01408
		caf [kg/kg]	0.1643
		λ (excess air fraction)	3.999
		$\eta_{I,cycle,max}$	**43.98**

Table 4. Optimization of the Performance of the Turboshaft Engine Cycle for the Maximum Exergy Efficiency ($\eta_{II,cycle,max}$) at Sea Level, RH_{amb}=15%, TIT=1200 ℃ and Different Ambient Temperatures.

T_{amb} [℃]	TIT [℃]	Design Parameters	Values
10	1200	$r_{p.comp}$	34.99
		far [kg/kg]	0.01596
		caf [kg/kg]	0.149
		λ (excess air fraction)	3.614
		$\eta_{II,cycle,max}$	**42.52**
25	1200	$r_{p.comp}$	34.99
		far [kg/kg]	0.01499
		caf [kg/kg]	0.1563
		λ (excess air fraction)	3.806
		$\eta_{II,cycle,max}$	**41.37**
40	1200	$r_{p.comp}$	34.99
		far [kg/kg]	0.01408
		caf [kg/kg]	0.1643
		λ (excess air fraction)	3.999
		$\eta_{II,cycle,max}$	**40.06**

Tables 3 and 4 show that both energy and exergy efficiencies will significantly increase with a decrease in air temperature because of the performance improvement of the compressor and entire cycle at lower inlet temperatures.

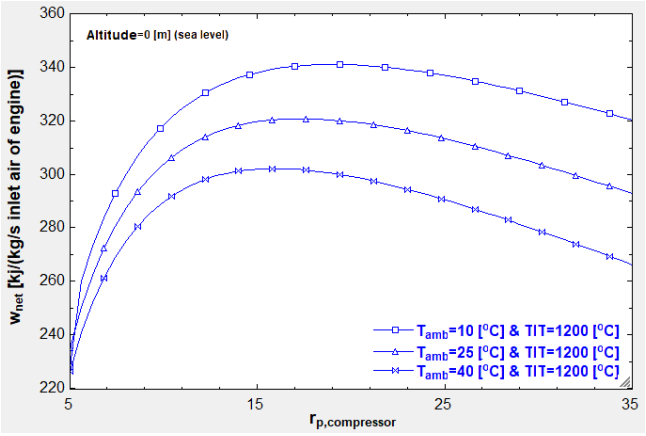

Figure 2. Change curve of w_{net} vs. $r_{p,comp}$ at sea level, RH_{amb}=15%, TIT =1200 ℃ and different ambient temperatures for turboshaft engine.

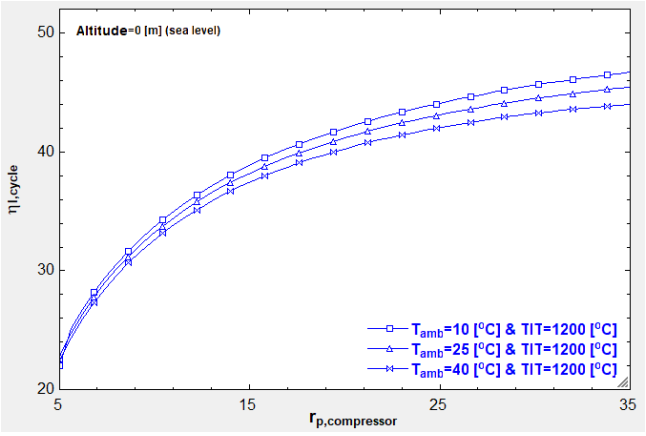

Figure 3. Change curve of thermal efficiency ($\eta_{I,cycle}$) vs. $r_{p,comp}$ at sea level, RH_{amb}=15%, TIT=1200 ℃ and different ambient temperatures for turboshaft engine.

In Figures 2, 3, and 4 the curves of different performance parameters of the turboshaft engine have been plotted versus changes of pressure ratio ($r_{p,comp}$). Results show that specific net-work (w_{net}), energy efficiency ($\eta_{I,cycle}$) and exergy efficiency ($\eta_{II,cycle}$) bear an indirect relationship with ambient temperature. Moreover, there is an optimum pressure ratio for the maximum net work because at the lower r_p the compressor work is small in comparison with the turbine work but as the r_p increases the slop of required compressor work exceeds the slop of work production by the turbine. The maximum w_{net} occurs around $r_{p,comp}$=17-18 (Figure 2), while $\eta_{I,cycle}$ and $\eta_{II,cycle}$ continuously increase for larger pressure ratios (Figures 3,4).

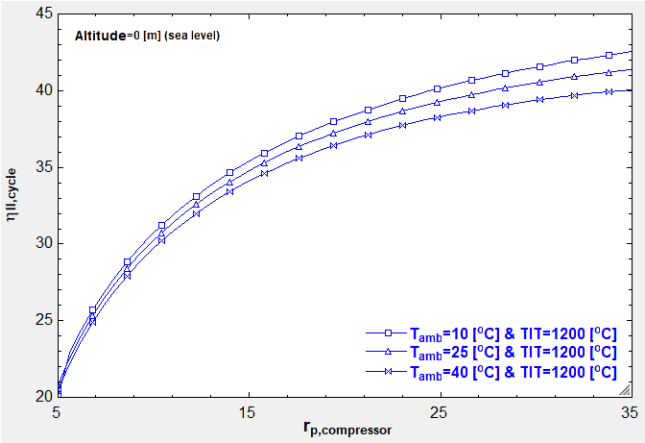

Figure 4. Change curve of exergy efficiency ($\eta_{II,cycle}$) vs. $r_{p,comp}$ at sea level, RH_{amb}=15%, TIT=1200 ℃ and different ambient temperatures for turboshaft engine.

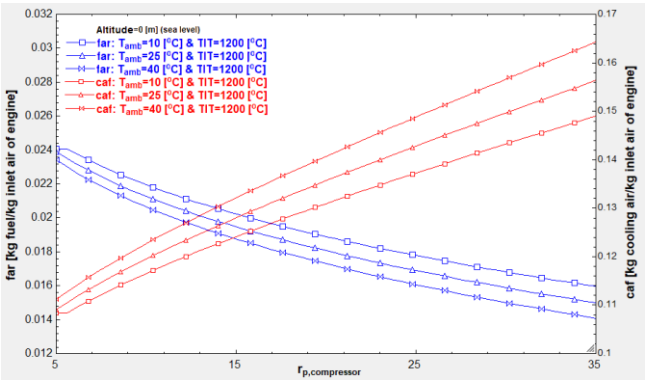

Figure 5. Change curves of caf and far vs. $r_{p,comp}$ at sea level, RH_{amb}=15%, TIT=1200 ℃ and different ambient temperatures for turboshaft engine.

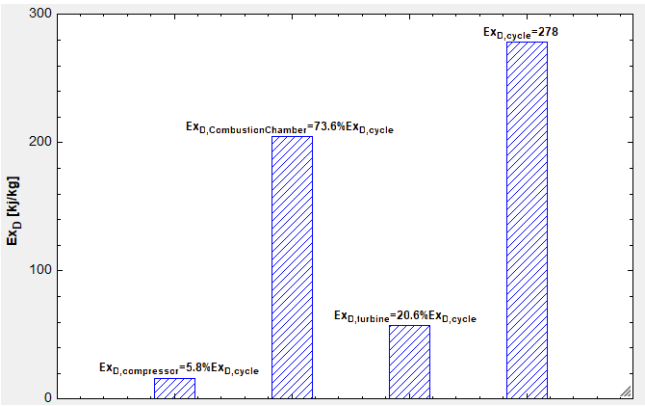

Figure 6. Bar plot of exergy destructions (Ex_D) of components at sea level, Tamb=25 ℃, RHamb=15%, TIT=1200 ℃ and $\eta_{II,max}$=41.37 for turboshaft engine.

Results also show that at sea level to obtain the same turbine inlet temperature (TIT), the fuel consumption (far) is increases by decreasing of the air temperatures. On the contrary, the decrease of air temperature enlarges the cooling capacity, consequently, the amount of required cooling air fraction (caf) for turbine blades decreases (Figure 5).

Figure 6 shows that in optimum exergy efficiency of the cycle the highest amount of exergy destruction (Ex_D) belongs to the combustion chamber (73%), followed by the turbine (21%) and compressor (6%).

Predictably, the highest amount of η_{II} belongs to the compressor (97%), followed by the turbine (94%) and combustion chamber (71%) as shown in Figure 7.

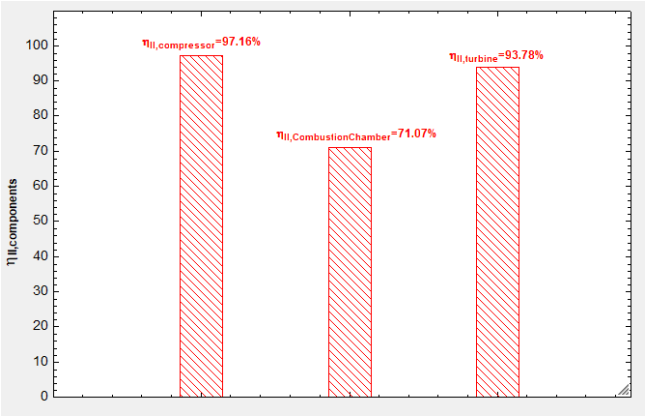

Figure 7. Bar plot of exergy efficiency (η_{II}) of components at sea level, RH_{amb}=15%, T_{amb} =25 ℃, TIT=1200 ℃ and $\eta_{II,max}$=41.37 for turboshaft engine.

In the following part, the performance analyses of turboshaft have been studied at different altitudes.

At different altitudes, both ambient air temperature and density play important roles in determining the performance of turboshaft engines. Knowing that specific altitude is accompanied by specific temperature and density, the performance has been calculated for different altitudes. By increasing the flight altitude from 6 km to 9 km, both the air temperature and density decreased (Table 5).

Table 5. Ambient air properties at different altitudes.

Altitude [m]	T_{amb} [℃]	P_{amb} [kPa]	ρ_{amb} [kg/m^3]
6000	-24.0	47.18	0.6597
9000	-43.5	30.74	0.4664

Table 6. Optimization of the Performance of the Turboshaft Engine Cycle for the Maximum Specific Work (w_{net}) at TIT=1200 ℃ and Different Altitudes.

Altitude [m]	TIT [℃]	Design Parameters	Values
6000	1200	$r_{p.comp}$	22.51
		far [kg/kg]	0.02032
		caf [kg/kg]	0.1238
		λ (excess air fraction)	2.926
		$w_{net,max}$ [kJ/kg]	**392.7**
9000	1200	$r_{p.comp}$	26.25
		far [kg/kg]	0.02085
		caf [kg/kg]	0.1214
		λ (excess air fraction)	2.86
		$w_{net,max}$ [kJ/kg]	**425.9**

The air temperature drop increases the required fuel mass to achieve the same turbine inlet temperature. On the other hand, decreasing the density of air decreases the inlet mass flow rate. The temperature drop with altitude-gain plays a dominant role rather than the density drop in the change of total mass flow rate. Consequently, the entire mass flow rate will increase with higher altitudes and lead to an increase in the specific net-work of the turboshaft (Table 6).

The results show that both energy and exergy efficiencies are slightly increasing with altitude gain (Tables 7 and 8).

Table 7. Optimization of the Performance of the Turboshaft Engine Cycle for the Maximum Thermal Efficiency ($\eta_{I,cycle,max}$) at TIT=1200 ℃ and Different Altitudes.

Altitude [m]	TIT [℃]	Design Parameters	Values
6000	1200	$r_{p.comp}$	34.99
		far [kg/kg]	0.01823
		caf [kg/kg]	0.1346
		λ (excess air fraction)	3.22
		$\eta_{I,cycle,max}$	**49.6**
9000	1200	$r_{p.comp}$	34.99
		far [kg/kg]	0.01956
		caf [kg/kg]	0.1276
		λ (excess air fraction)	3.027
		$\eta_{I,cycle,max}$	**50.2**

Table 8. Optimization of the Performance of the Turboshaft Engine Cycle for the Maximum Exergy Efficiency ($\eta_{II,cycle,max}$) at TIT=1200 ℃ and Different Altitudes.

Altitude [m]	TIT ℃	Design Parameters	Values
6000	1200	$r_{p.comp}$	34.99
		far [kg/kg]	0.01823
		caf [kg/kg]	0.1346
		λ (excess air fraction)	3.22
		$\eta_{II,cycle,max}$	**44.69**
9000	1200	$r_{p.comp}$	34.99
		far [kg/kg]	0.01956
		caf [kg/kg]	0.1276
		λ (excess air fraction)	3.027
		$\eta_{II,cycle,max}$	**45.73**

Figures 8, 9, and 10 show that the performance values of turboshaft engine of w_{net}, $\eta_{I,cycle}$ and $\eta_{II,cycle}$ increase with altitude gain from 6 km to 9 km.

The maximum w_{net} for 6 km and 9 km altitudes occurs at $r_{p,comp}$=22.5 and 26.2, respectively (Figures 8, 9), while $\eta_{I,cycle}$ and $\eta_{II,cycle}$ continuously increase for larger pressure ratios (Figure 10).

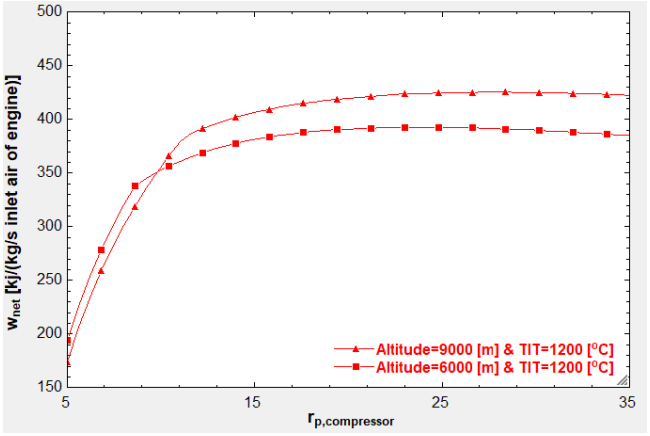

Figure 8. Change curve of w_{net} vs. $r_{p,comp}$ at TIT=1200 ℃ and different altitudes for turboshaft engine.

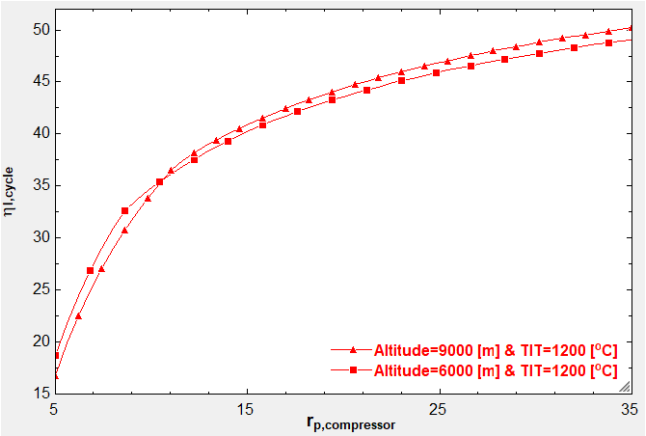

Figure 9. Change curve of thermal efficiency ($\eta_{I,cycle}$) at TIT=1200 ℃ and different altitudes for turboshaft engine.

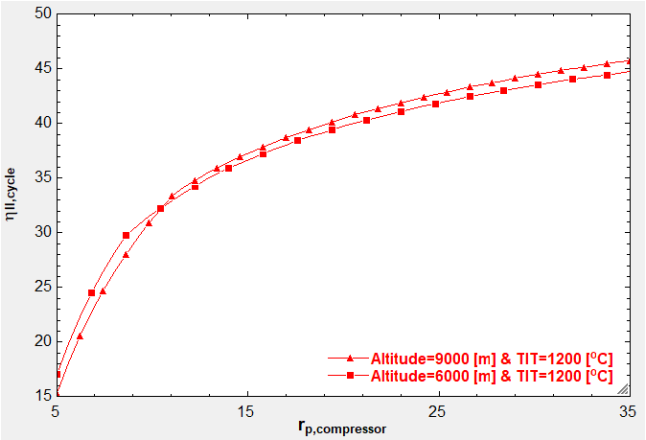

Figure 10. Change curve of exergy efficiency ($\eta_{II,cycle}$) at TIT=1200 ℃ and different altitudes for turboshaft engine.

Knowing that ambient temperature and density bear different influences on the fuel consumption and cooling air fraction, at the beginning the far and caf does not significantly change with increasing r_p. After a specific point, the larger r_p will result in the decrease of far and increase of caf. Moreover, far and caf bear a direct and indirect relationship with altitude gain (Figure 11).

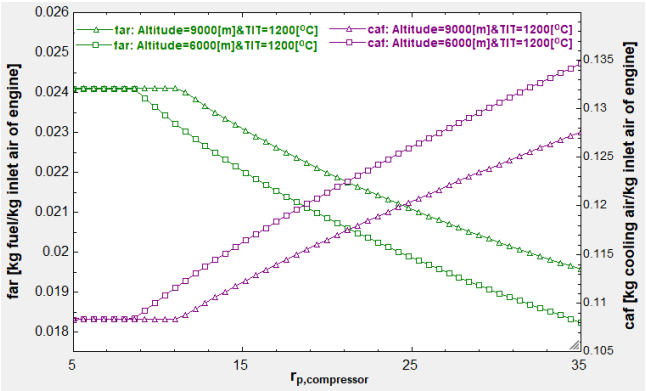

Figure 11. Change curves of caf and far vs. $r_{p,comp}$ at TIT=1200 ℃ and different altitudes for turboshaft engine.

Figure 12 shows that at 9 km altitude and for optimum exergy efficiency about 4%, 80%, and 16% of entire cycle exergy-destructions occur in the compressor, combustion chamber, and turbine, respectively. The highest amount of Ex_D belongs to the combustion chamber, followed by the turbine and compressor.

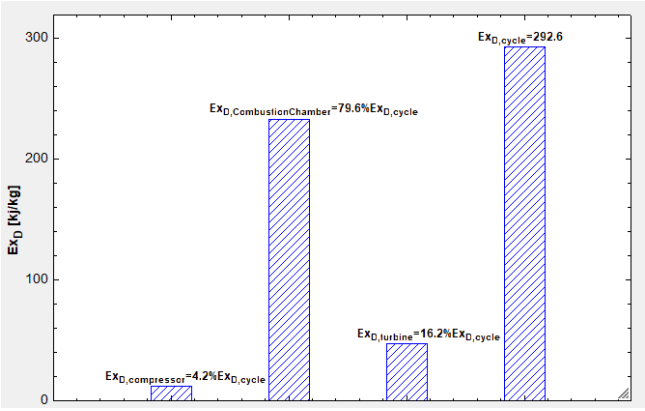

Figure 12. Bar plot of exergy destructions (Ex_D) of components at altitude 9000 m, TIT=1200 ℃ and $\eta_{II,max}$=45.73 for turboshaft engine.

The highest amount of η_{II} belongs to the compressor (97%), followed by the turbine (94%) and combustion chamber (74%) at 9 km altitude as shown in Figure 13.

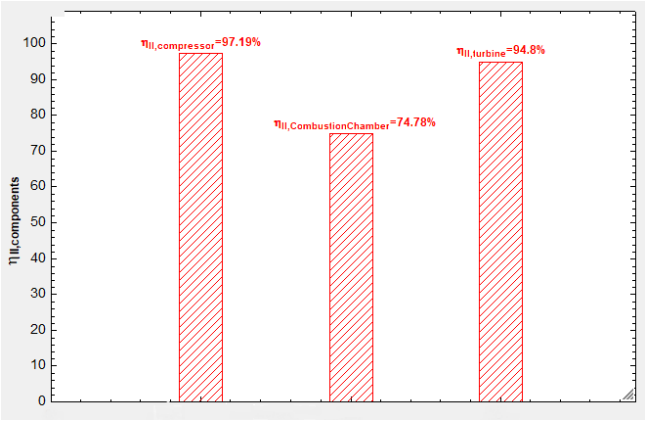

Figure 13. Bar plot of exergy efficiency (η_{II}) of components at altitude 9000 m, TIT=1200 ℃ and $\eta_{II,max}$=45.73 for turboshaft engine.

5. Conclusion

The thermodynamics optimization and energy-exergy analyses have been done for a turboshaft engine equipped with turbine blades' cooling in different ambient air conditions at different flight altitudes. Results show that:

At the sea level:

- The temperature of ambient air plays an important role in the performance of the turboshaft engine.
- The temperature drop will lead to significant increase in the specific net-work, energy and exergy efficiencies of the cycle.
- In optimum exergy efficiency of entire cycle about 6%, 73%, and 21% of entire cycle exergy-destructions occurs in the compressor, combustion chamber and turbine, respectively. The highest exergy destruction belongs to the combustion chamber, followed by the turbine and compressor.
- The highest exergy efficiency belongs to the compressor (97%), followed by the turbine (94%) and combustion chamber (71%).

At high altitudes:

- The inlet air temperature and density respectively bear indirect and direct relationships with the specific net-work of the turboshaft engine.

- The temperature drop of ambient air plays dominant role and lead to a major increase in the specific net-work of the turboshaft engine with altitude gain from 6 km to 9 km.
- Both energy and exergy efficiencies are slightly increasing with altitude gain.
- At 9 km altitude and for optimum exergy efficiency of entire cycle about 4%, 80%, and 16% of entire cycle exergy-destructions occur in the compressor, combustion chamber, and turbine, respectively. Again, the highest exergy destruction belongs to the combustion chamber, followed by the turbine and compressor.
- The highest exergy efficiency belongs to the compressor (97%), followed by the turbine (94%) and combustion chamber (74%) at 9 km altitude.

For all flight scenarios:

- The fuel consumption is larger for lower air temperatures to achieve the same turbine inlet temperature.
- On the contrary, the decrease in air temperature enlarges the cooling capacity, consequently, the cooling air fraction required for turbine blades decreases.

Nomenclature

c_p	specific heat capacity at constant pressure	KJ/ Kg.K
e	specific energy	KJ/ Kg
ex	specific exergy	KJ/ Kg
g	gravitational acceleration constant	m/s^2
$\dot{I}$	irreversibilities	kJ/s
M	Molar Mass	gram/mole
$\dot{m}$	mass flow rate	kg/s
P_0	ambient pressure	Pa
P	pressure	Pa
$\dot{Q}$	Heat flux	kJ/s
r_P	Dimensionless pressure ratio	unitless
s	specific entropy	kJ/kg
t	time	s
T	temperature	K
T_0	ambient temperature	K
V	velocity	m/s
$\dot{W}$	Work flux	kJ/s

Greek Symbols

η	Dimensionless efficiency	unitless
λ	Dimensionless excess air	unitless
ρ	density	Kg

Subscripts

I	1st Law or energetic
II	2nd Law or exergetic
air	ambient air
cc	combustion chamber
ch	chemical
comp	compressor
D	destruction
e	exit
i	input
in	inlet
k	kinetic
p	potential
ph	physical
poly	polytropic
Q	thermal
r	rotator
turb	turbine

Abbreviations

caf	cooling air fraction
CIT	compressor inlet temperature
COT	compressor outlet temperature
far	fuel air ratio
TIT	turbine inlet temperature
TOT	turbine outlet temperature

Appendices

Appendix A. Energy Analysis

Appendix A.1 Mass Conservation (Continuity)

$$\frac{dm}{dt} = \sum \dot{m}_i - \sum \dot{m}_e \quad \text{(A. 1)}$$

which $\dot{m}_i$ and $\dot{m}_e$ are the inlet and outlet mass flow rates, respectively.

Appendix A. 2 Energy Conservation (1st Law of Thermodynamics)

$$\frac{dE}{dt} = \dot{Q} - \dot{W} + \sum \dot{m}_i e_i - \sum \dot{m}_e e_e \quad \text{(A. 2)}$$

which $\dot{E} = \dot{m}(e)$ and $\dot{Q}$, $\dot{W}$, and e are heat, work, and specific energy, respectively.

$$e = h + \frac{V^2}{2} + gz \quad \text{(A. 3)}$$

h, $\frac{v^2}{2}$ and gz are specific enthalpy, kinetic and potential energy terms, respectively.

Appendix A. 3 Entropy Balance (2nd Law of Thermodynamics)

$$\frac{dS}{dt} = \sum_{i=1}^{N} \frac{\dot{Q}_i}{T_i} + \sum \dot{m}_i s_i - \sum \dot{m}_e s_e + \delta\dot{S}_{gen} \quad \text{(A. 4)}$$

which $\dot{S} = \dot{m}(s)$, and s is specific entropy.
By restating of this entropy equation, the entropy generation is:

$$\delta\dot{S}_{gen} = \frac{dS}{dt} + \sum \dot{m}_e s_e - \sum \dot{m}_i s_i - \sum_{i=1}^{N} \frac{\dot{Q}_i}{T_i} \quad \text{(A. 5)}$$

Based on the Gouy–Stodola theorem, for a control volume with the ambient temperature of T0, the irreversibilities value is calculated as:

$$\dot{I} = T_0 \, \delta\dot{S}_{gen} \quad \text{(A. 6)}$$

Appendix A. 4 State Equation

The additional equations like state equation of ideal gas, isentropic and polytropic formulas for compressor and turbine efficiencies may be applied to solve the thermodynamic problems.
For the steady state steady flow (SSSF) thermodynamic processes, all the temporal terms equal zero ($\frac{d}{dt} = 0.0$).

Appendix A. 5 Energy or thermal efficiency (1st law efficiency)

$$\eta_I = \eta_{thermal} = \frac{\dot{E}_{benefited}}{\dot{E}_{cost}} \quad \text{(A. 7)}$$

When the energy analysis is done, all unknowns (thermodynamic properties) of the cycle are calculated.

Then, simply the exergy analysis is implemented by using the new exergetic definitions of the components and entire cycle.

Appendix B. Exergy Analysis

Appendix B. 1 The Concept of Exergy

$$\text{Energy}=\text{Exergy}+\text{Anergy} \quad \text{(B. 1)}$$

which exergy and anergy are maximum accessible work and non-accessible work, respectively.

Appendix B. 2 Definition of the Environment from the Exergy Analysis Point of View

From the point of view of exergy analysis, the environment of a system is completely in a thermodynamic equilibrium. There are no gradients in the environment, including pressure, temperature, and chemical potential gradients. In addition, it is not possible to obtain work from the interaction of different components of the environment with each other. Therefore, in exergy analysis, the environment is a reference used to evaluate the performance potential of different systems.

The restricted dead state is a state of the substance in which it is in thermal and mechanical equilibrium with the environment. However, they are not in chemical equilibrium with each other. In the restricted dead state, the substance's temperature and pressure are equal to the ambient temperature and pressure, and the velocity and potential energy of the substance are zero. The dead state is a state of the substance in which it is not only in thermal and mechanical equilibrium but also in chemical equilibrium with the surrounding environment.

Appendix B. 3 Restricted Dead State and Dead State

The restricted dead state is a state of the substance in which it is in thermal and mechanical equilibrium with the environment. However, they are not in chemical equilibrium with each other. In the restricted dead state, the substance's temperature and pressure are equal to the ambient temperature and pressure, and the velocity and potential energy of the substance are zero.

The dead state is a state of the substance in which it is not only in thermal and mechanical equilibrium but also in chemical equilibrium with the surrounding environment.

Appendix B. 4 Exergy Balance

For each component:

$$\frac{dEx}{dt}=\dot{Q}\left(1-\frac{T_0}{T}\right)-\dot{W}+\sum \dot{m}_i\, ex_i-\sum \dot{m}_e\, ex_e+\dot{E}x_D \quad \text{(B. 2)}$$

which $\dot{E}x = \dot{m}(ex)$, and $\dot{E}x_D$ is the exergy destruction of a component defined as:

$$\dot{E}x_D=\dot{I}=T_0\,\delta\dot{S}_{gen}=T_0\,(\dot{m}\,\delta s_{gen}) \quad \text{(B. 3)}$$

which $\dot{I}$ is the irreversibilities value and $\delta\dot{S}_{gen}$ is the entropy generation of a thermodynamic process because of irreversibilities.

For the entire cycle:

$$\frac{dEx}{dt}=\dot{Q}\left(1-\frac{T_0}{T}\right)-\dot{W}+\sum \dot{m}_i\, ex_i-\sum \dot{m}_e\, ex_e+\dot{E}x_{D,cycle}+\dot{E}x_{D,loss} \quad \text{(B. 4)}$$

which $\dot{E}x_{D,cycle}$ is the total exergy destruction of a cycle, and $\dot{E}x_{D,loss}$ is the exergy loss due to the exhaust which is defined as:

$$\dot{E}x_{D,loss}=\dot{m}_{exhaust}\, \dot{ex}_{exhaust} \quad \text{(B. 5)}$$

Again, for the steady state steady flow (SSSF) thermodynamic processes, all the temporal terms equal zero ($\frac{d}{dt}=0.0$).

Appendix B. 5 Exergy Types

In the absence of the effects of nuclear, magnetic, electric, and surface tension fields, the exergy can be written as a summation of physical, chemical, kinetic, potential, and heat transfer exergy parts as:

$$\dot{E}x=\dot{E}x_{ph}+\dot{E}x_{ch}+\dot{E}x_k+\dot{E}x_p+\dot{E}x_Q \quad \text{(B. 6)}$$

The physical exergy ($\dot{E}x_{ph}$) is the maximum accessible work that a substance can do in a reversible process which a substance goes from its initial state to the restricted dead state as:

$$Ex_{ph}=(h-h_0)-T_0(s-s_0) \quad \text{(B. 7)}$$

The chemical exergy ($\dot{E}x_{ch}$) is the amount of accessible work a substance can do in the chemical equilibrium process surrounded by an environment in which a substance goes from the restricted dead state to the dead state. One of the important applications of the concept of chemical exergy is the calculation of fuel exergy. For hydrocarbon fuels with the form C_nH_m, the amount of chemical exergy is obtained from:

$$Ex_{ch}=-\Delta g(T_0,P_0)+T_0R\,\ln\left[\frac{(y_{0,O_2})^{n+\frac{m}{4}}}{(y_{0,CO_2})^{n}\,(y_{0,H_2O})^{m}}\right] \quad \text{(B. 8)}$$

which R, y, g are the universal gas constant, molar fraction, and Gibbs function, respectively, and:

$$-\Delta g(T_0,P_0)=g(T_0,P_0)_{C_nH_m}-n\,g(T_0,P_0)_{CO_2}-\frac{m}{2}\,g(T_0,P_0)_{H_2O} \quad \text{(B. 9)}$$

The chemical exergy of a mixture of ideal gases can be obtained from the following equation:

$$Ex_{ch}=T_0\,R\,\sum y_i \ln\left(\frac{y_i}{y_{0,i}}\right) \quad \text{(B. 10)}$$

The kinetic exergy of equation ($\dot{E}x_k$) can be calculated as:

$$Ex_k=m\,\frac{V^2}{2} \quad \text{(B. 11)}$$

The potential exergy of equation ($\dot{E}x_p$) can be obtained as:

$$Ex_p=m\,g\,z \quad \text{(B. 12)}$$

The exergy of heat transfer ($\dot{E}x_Q$) is the maximum work that can be obtained from the thermal energy transfer as:

$$Ex_Q = Q\left(1-\frac{T_0}{T}\right) \quad \text{(B. 13)}$$

Appendix B. 6 Exergy Efficiency (2nd Law Efficiency)

$$\eta_{II} = \frac{\sum \dot{E}x_{benefited}}{\sum \dot{E}x_{in}} = 1-\frac{\sum \dot{E}x_D}{\sum \dot{E}x_{in}} \quad \text{(B. 14)}$$

Appendix C. Equations

Table C. 1. Equations for Energy-Exergy Analyses.

Components	Related Equations
Compressor	$\dot{m}_2=(1-caf)\dot{m}_1$ $\dot{W}_{comp}=\dot{m}_1(e_2-e_1)$ $\eta_{I,comp}=\eta_{poly,comp}=\frac{\bar{R}T\frac{dP}{P}}{\bar{C}_{p,air}dT}$ $\dot{E}x_{D,comp}=\dot{W}_{comp}+\dot{m}_1ex_1-\dot{m}_2ex_2$ $\eta_{II,comp}=\frac{(\dot{W}_{comp}-\dot{E}x_{D,comp})}{\dot{W}_{comp}}100$
Cooling Air Fraction	$T_r=0.8451TIT+136.2$, T_r and TIT are in ℃. $caf=\frac{2(1+far)(e_3-e_r)}{(2e_3-e_2-e_r)}$
Combustion Chamber	$\dot{m}_3=\dot{m}_2+\dot{m}_f$, which $\dot{m}_f=(far)\dot{m}_1$ $\int_{298.15}^{T_f}\bar{C}_{p,C_nH_m}dT+\lambda\left(n+\frac{m}{4}\right)\int_{298.15}^{T_2}\bar{C}_{p,O_2}dT+$ $\lambda\left(n+\frac{m}{4}\right)3.76\int_{298.15}^{T_2}\bar{C}_{p,N_2}dT+$ $\lambda\left(n+\frac{m}{4}\right)4.76\bar{\omega}_1\int_{298.15}^{T_2}\bar{C}_{p,H_2O}dT=$ $n\int_{298.15}^{TIT}\bar{C}_{p,CO_2}dT+(\lambda-1)\left(n+\frac{m}{4}\right)\int_{298.15}^{TIT}\bar{C}_{p,O_2}dT+$ $3.76\lambda\left(n+\frac{m}{4}\right)\int_{298.15}^{TIT}\bar{C}_{p,N_2}dT+$ $\left[\lambda\left(n+\frac{m}{4}\right)(4.76\bar{\omega}_1)+\frac{m}{2}\right]\int_{298.15}^{TIT}\bar{C}_{p,H_2O}dT$ $far=\frac{M_{C_nH_m}}{\lambda\left(n+\frac{m}{4}\right)4.76(1+\bar{\omega}_1)M_{air}\eta_{I,cc}}(1-caf)$ $\dot{E}x_{D,cc}=\dot{m}_2ex_2+\dot{m}_fex_f-\dot{m}_3ex_3$ $\eta_{II,cc}=\left[1-\frac{\dot{E}x_{D,cc}}{(far)\dot{m}_1ex_f}\right]100$
Turbine	$\dot{m}_4=(1+far)\dot{m}_1$ $\dot{W}_{turb}=(caf)\dot{m}_1e_2+\dot{m}_3e_3-\dot{m}_4e_4$ $\eta_{I,turb}=\eta_{poly,turb}=\frac{\bar{C}_{p,g}dT}{\bar{R}T\frac{dP}{P}}$ $\dot{E}x_{D,turb}=\dot{m}_3ex_3+(caf)\dot{m}_1ex_2-\dot{m}_4ex_4-\dot{W}_{turb}$ $\eta_{II,turb}=\frac{\dot{W}_{turb}}{(\dot{W}_{turb}+\dot{E}x_{D,turb})}100$
Cycle	$\dot{W}_{net}=(\dot{W}_{turb}-\dot{W}_{comp})\eta_{mech}$ $\eta_{I,cycle}=\frac{\dot{W}_{net}}{(far)\dot{m}_1\,LHV}100$ $\dot{E}x_{D,cycle}=\dot{E}x_{D,comp}+\dot{E}x_{D,cc}+\dot{E}x_{D,turb}$ $\eta_{II,cycle}=\frac{\dot{W}_{net}}{(far)\dot{m}_1\,ex_f}100$

References:

[1] K. Coban, C. O. Colpan, and T. H. Karakoc, "Application of thermodynamic laws on a military helicopter engine," *Energy*, vol. 140, pp. 1427–1436, 2017.

[2] V. Zare, S. Khodaparast, and E. Shayan, "Comparative thermoeconomic analysis of using different jet fuels in a turboshaft engine for aviation applications," *AUT Journal of Mechanical Engineering*, vol. 5, no. 2, pp. 297–312, 2021.

[3] A. Bejan and D. L. Siems, "The need for exergy analysis and thermodynamic optimization in aircraft development," *Exergy, An International Journal*, vol. 1, no. 1, pp. 14–24, 2001.

[4] E. Koruyucu, O. Altuntas, and T. H. Karakoc, "Exergetic investigation of a turboshaft helicopter engine related to engine power," *SAE International Journal of Aerospace*, vol. 13, no. 01-13-02-0019, pp. 257–267, 2020.

[5] O. Balli, "Exergetic, sustainability and environmental assessments of a turboshaft engine used on helicopter," *Energy*, vol. 276, p. 127593, 2023.

[6] G. Tsatsaronis, "Strengths and limitations of exergy analysis," in *Thermodynamic optimization of complex energy systems*, A. Bejan and E. Mamut, Ed., New York, NY, USA, Springer, 1999, pp. 93–100.

[7] I. Dincer and M. A. Rosen, *Exergy: energy, environment and sustainable development*, Oxford, U.K., Elsevier, 2012.

[8] D. Riggins and C. Clinton, "Thrust modeling for hypersonic engines," presented at the International Aerospace Planes and Hypersonics Technologies, Chattanooga, TN, USA, Apr. 3–7, 1995, p. 6081.

[9] D. Riggins, "High-speed engine/component performance assessment using exergy and thrust-based methods," NASA Technical Reports Server, USA, Tech. Rep. NASA CR-198271, 1996.

[10] D. Riggins, "The evaluation of performance losses in multi-dimensional propulsive flows," presented at the 34th Aerospace Sciences Meeting and Exhibit, Missouri, Rolla Univ., USA, Jan. 15–18, 1996, p. 375.

[11] D. Riggins, "Brayton cycle engine/component performance assessment using energy and thrust-based methods," presented at the 32nd Joint Propulsion Conference and Exhibit, Missouri, Rolla Univ., USA, Jul. 15–18, 1996, p. 2922.

[12] D. W. Riggins, "Evaluation of performance loss methods for high-speed engines and engine components," *Journal of Propulsion and Power*, vol. 13, no. 2, pp. 296–304, 1997.

[13] D. Riggins, "The thermodynamic continuum of jet engine performance: the principle of lost work due to irreversibility in aerospace systems," *International Journal of Thermodynamics*, vol. 6, no. 3, pp. 107–120, 2003.

[14] D. W. Riggins, T. Taylor, and D. J. Moorhouse, "Methodology for performance analysis of aerospace vehicles using the laws of thermodynamics," *Journal of Aircraft*, vol. 43, no. 4, pp. 953–963, 2006.

[15] E. T. Curran and R. R. Craig, "The use of stream thrust concepts for the approximate evaluation of hypersonic ramjet engine performance," Wright-Patterson Air Force Aero Propulsion Laboratory, Dayton, OH, USA, Tech. Rep. AFAPL-TR-73-38, 1973.

[16] H. Brilliant, "Analysis of scramjet engines using exergy methods," presented at the 31st Joint Propulsion

Conference and Exhibit, San Diego, CA, USA, Jul. 10–12, 1995, p. 2767.

[17] J. Horlock, "Thermodynamic availability and propulsion," *American Institute of Aeronautics and Astronautics*, vol. 6, pp. 99–741, 1999.

[18] J. Etele and M. A. Rosen, "The impact of reference environment selection on the exergy efficiencies of aerospace engines," presented at the ASME International Mechanical Engineering Congress and Exposition, vol. 16509, Nashville, Tennessee, USA, Nov. 14–19, 1999, pp. 583–591.

[19] M. A. Rosen and J. Etele, "Aerospace systems and exergy analysis: applications and methodology development needs," *International Journal of Exergy*, vol. 1, no. 4, pp. 411–425, 2004.

[20] D. L. Hunt, R. M. Cummings, and M. B. Giles, "Wake integration for three-dimensional flowfield computations: Applications," *Journal of aircraft*, vol. 36, no. 2, pp. 366–373, 1999.

[21] M. B. Giles and R. M. Cummings, "Wake integration for three-dimensional flowfield computations: theoretical development," *Journal of aircraft*, vol. 36, no. 2, pp. 357–365, 1999.

[22] D. Moorhouse, H. Charles, and J. Prendergast, "Thermal analysis of hypersonic inlet flow with exergy-based design methods," *International Journal of Thermodynamics*, vol. 5, no. 4, pp. 161–168, 2002.

[23] K. A. B. Pathirathna, "Gas turbine thermodynamic and performance analysis methods using available catalog data," M.Sc. thesis, Dept. Engineering and Sustainable Development, Univ. Gävle, Gävle, Sweden, 2013. [Online].Available:https://avys.omu.edu.tr/storage/app/public/ozcanh/111428/MMB718-3.pdf

[24] V. Amati, C. Bruno, D. Simone, and E. Sciubba, "Exergy analysis of hypersonic propulsion systems: Performance comparison of two different scramjet configurations at cruise conditions," *Energy*, vol. 33, no. 2, pp. 116–129, 2008.

[25] D. F. Rancruel and M. R. von Spakovsky, "Decomposition with thermoeconomic isolation applied to the optimal synthesis/design and operation of an advanced tactical aircraft system," *Energy*, vol. 31, no. 15, pp. 3327–3341, 2006.

[26] E. T. Turgut, T. H. Karakoc, and A. Hepbasli, "Exergoeconomic analysis of an aircraft turbofan engine," *International Journal of Exergy*, vol. 6, no. 3, pp. 277–294, 2009.

[27] M. Fallah, A. Sohrabi, and N. H. Mokarram, "Proposal and energy, exergy, economic, and environmental analyses of a novel combined cooling and power (ccp) system," *Journal of the Brazilian Society of Mechanical Sciences and Engineering*, vol. 45, no. 9, p. 441, 2023.

[28] G. C. Oates, *Aerothermodynamics of gas turbine and rocket propulsion*, Reston, VA, USA, AIAA, 1997.

[29] J. D. Mattingly, K. M. Boyer, and H. von Ohain, *Elements of propulsion: gas turbines and rockets*, Reston , VA, USA, AIAA, 2006.

[30] R. Langton and B. MacIsaac, *Gas turbine propulsion systems*, Hoboken, NJ, USA, John Wiley & Sons, 2011.

[31] A. F. El-Sayed, *Fundamentals of aircraft and rocket propulsion*, London, U.K., Springer, 2016.

[32] A. F. El-Sayed, *Aircraft propulsion and gas turbine engines*, Boca Raton, FL, USA, CRC press, 2017.

[33] J. Van Wylen and E. Sonntag, *Fundamental of Classical Thermodynamics*, Hoboken, NJ, USA, John Wiley & Sons, 1998.

[34] K. Annamalai, I. K. Puri, and M. A. Jog, *Advanced thermodynamics engineering*, Boca Raton, FL, USA, CRC press, 2010.

[35] D. Winterbone and A. Turan, *Advanced thermodynamics for engineers*, Oxford, U.K., Butterworth-Heinemann, 2015.

[36] A. Bejan, *Advanced engineering thermodynamics*, Hoboken, NJ, USA, John Wiley & Sons, 2016.

[37] M. Tabatabaian, *Advanced Thermodynamics*, Herndon, VA, USA, Mercury Learning & Information, 2017.

[38] C. Borgnakke and R. E. Sonntag, *Fundamentals of thermodynamics*, Hoboken, NJ, USA, John Wiley & Sons, 2022.

[39] M. Yari and K. Sarabchi, "Comparative investigation of various humidified gas turbine cycles," presented at the Turbo Expo: Power for Land, Sea, and Air, ASME, vol. 41723, Vienna, Austria, Jun. 14–17, 2004, pp. 693–703.

[40] K. Sarabchi, "Performance evaluation of reheat gas turbine cycles," *Proceedings of the Institution of Mechanical Engineers*, Part A: Journal of Power and Energy, vol. 218, no. 7, pp. 529–539, 2004.

[41] M. Fallah, H. Siyahi, R. A. Ghiasi, S. Mahmoudi, M. Yari, and M. Rosen, "Comparison of different gas turbine cycles and advanced exergy analysis of the most effective," *Energy*, vol. 116, pp. 701–715, 2016.

[42] P. Charbonneau, "An introduction to genetic algorithms for numerical optimization," *NCAR Technical Note,* vol. 74, pp. 4–13, 2002.